Molecular Biology of the Cell
Vol. 13, 2334–2346, July 2002

Small GTP-binding Protein TC10 Differentially Regulates Two Distinct Populations of Filamentous Actin in 3T3L1 Adipocytes[V]

Makoto Kanzaki,* Robert T. Watson,* June Chunqiu Hou,* Mark Stamnes,* Alan R. Saltiel,† and Jeffrey E. Pessin*‡

*Department of Physiology and Biophysics, The University of Iowa, Iowa City, Iowa 52242; and †Departments of Internal Medicine and Physiology, Life Sciences Institute, The University of Michigan Medical Center, Ann Arbor, Michigan 48109

Submitted October 10, 2001; Received March 6, 2002; Accepted March 28, 2002
Monitoring Editor: David Drubin

TC10 is a member of the Rho family of small GTP-binding proteins that has previously been implicated in the regulation of insulin-stimulated GLUT4 translocation in adipocytes. In a manner similar to Cdc42-stimulated actin-based motility, we have observed that constitutively active TC10 (TC10/Q75L) can induce actin comet tails in *Xenopus* oocyte extracts in vitro and extensive actin polymerization in the perinuclear region when expressed in 3T3L1 adipocytes. In contrast, expression of TC10/Q75L completely disrupted adipocyte cortical actin, which was specific for TC10, because expression of constitutively active Cdc42 was without effect. The effect of TC10/Q75L to disrupt cortical actin was abrogated after deletion of the amino terminal extension (ΔN-TC10/Q75L), whereas this deletion retained the ability to induce perinuclear actin polymerization. In addition, alteration of perinuclear actin by expression of TC10/Q75L, a dominant-interfering TC10/T31N mutant or a mutant N-WASP protein (N-WASP/ΔVCA) reduced the rate of VSV G protein trafficking to the plasma membrane. Furthermore, TC10 directly bound to Golgi COPI coat proteins through a dilysine motif in the carboxyl terminal domain consistent with a role for TC10 regulating actin polymerization on membrane transport vesicles. Together, these data demonstrate that TC10 can differentially regulate two types of filamentous actin in adipocytes dependent on distinct functional domains and its subcellular compartmentalization.

INTRODUCTION

TC10 is a member of the Rho family of GTP-binding proteins and is closely related to Cdc42 (Neudauer *et al.*, 1998). Although TC10 is primarily expressed in adipose and muscle tissue (Neudauer *et al.*, 1998; Imagawa *et al.*, 1999), its function has only been peripherally examined. In vitro binding assays have indicated that active GTP-bound TC10 can bind a number of potential effectors, including mixed lineage kinase 2, myotonic dystrophy-related Cdc42 kinase, p21-activated protein kinases, the Borg family of interacting proteins, the mammalian partition-defective homolog Par6, and the N-WASP isoform of the Wiskott-Aldrich Syndrome Protein (Neudauer *et al.*, 1998; Joberty *et al.*, 1999, 2000). However, whether TC10 can interact with any of these potential effectors under physiological conditions has yet to be established. Nevertheless, similar to other members of the Rho family, expression of a constitutively active TC10 mutant (TC10/Q75L) in fibroblasts decreased actin stress fibers concomitant with the formation of plasma membrane microspikes (Murphy *et al.*, 1999). However, expression of wild-type TC10 (TC10/WT) was without any effect on fibroblast cell morphology or actin structures. In contrast, expression of wild-type Cdc42 (Cdc42/WT) or a constitutively active Cdc42 mutant (Cdc42/Q61L) in fibroblasts decreased actin stress fibers in parallel with the induction of actin protrusions and lamellipodia (Coghlan *et al.*, 2000). These data indicate that although fibroblasts express the necessary downstream effectors to modulate actin structure and are fully capable of activating Cdc42, they do not contain the endogenous machinery necessary to activate TC10, suggesting that TC10 function may be cell type specific.

We have recently observed that insulin can activate a signaling pathway leading to the activation of TC10 in adipocytes (Baumann *et al.*, 2000; Chiang *et al.*, 2001). This

Article published online ahead of print. Mol. Biol. Cell 10.1091/mbc.01–10–0490. Article and publication date are at www.molbiolcell.org/cgi/doi/10.1091/mbc.01–10–0490.

‡ Corresponding author. E-mail address: jeffrey-pessin@uiowa.edu.

[V] Online version of this article contains video material. Online version is available at www.molbiolcell.org.

apparently results from the insulin-dependent tyrosine phosphorylation of the Cbl protooncogene product, and its recruitment to a lipid raft plasma membrane microdomain via the adapter protein Cbl-associated protein. Once translocated, the tyrosine phosphorylated Cbl can recruit the SH2 adapter protein CrkII to lipid rafts. Because CrkII forms a stable complex with the guanylnucleotide exchange factor C3G, this protein is also targeted to this plasma membrane microdomain in response to insulin, where it converts the inactive GDP-bound TC10 protein to the GTP-bound activated state. Importantly, overexpression of TC10 was found to specifically inhibit the insulin-stimulated translocation of the GLUT4 protein from intracellular storage sites to the plasma membrane.

Recently, several studies have also suggested a role for actin in insulin-stimulated GLUT4 translocation. For example, treatment with the actin-depolymerizing agent cytochalasin D or the actin monomer binding Red Sea Sponge toxins latrunculin A or B inhibited insulin-stimulated GLUT4 translocation (Tsakiridis *et al.*, 1998; Wang *et al.*, 1998; Omata *et al.*, 2000). Importantly, differentiated adipocytes are large, round, lipid-laden cells and do not contain typical stress fibers, lamellipodia, or ruffling actin but instead display a cortical actin meshwork beneath the plasma membrane. In addition, the fact that TC10 is normally expressed in insulin-responsive tissues but not fibroblasts, coupled with our recent observation that insulin activates TC10 in adipocytes, prompted us to investigate the potential role of TC10 in the regulation of actin dynamics. In this article, we demonstrate that TC10 exerts two distinct effects in adipocytes, depolymerizing cortical F-actin beneath the plasma membrane and greatly increasing F-actin polymerization in the perinuclear region. This latter function is dependent upon N-WASP and mediates secretory membrane trafficking through the engagement of actin with COPI vesicle coat proteins.

MATERIALS AND METHODS

Materials

Clostridum difficile toxin B was obtained from Techlab (Blacksburg, VA) and latrunculin B was purchased from Calbiochem (La Jolla, CA). Texas Red-conjugated donkey anti-rabbit IgG, Cy5-conjugated donkey anti-mouse IgG, and fluorescein isothiocyanate-conjugated donkey anti-sheep IgG were purchased from Jackson Immunoresearch Laboratories (West Grove, PA). Rhodamine-phalloidin, rhodamine-actin, and the pACTIN-enhanced yellow fluorescent protein were purchased from Sigma-Aldrich (St. Louis, MO), Cyoskeleton (Denver, CO), and CLONTECH (Palo Alto, CA), respectively. β-COP antibody was obtained from Sigma-Aldrich. γ-COP antibody was a gift from Dr. F. Wieland (Ruprecht-Karls Universitat, Heidelberg, Germany). pKH3-TC10/WT, -TC10/Q75L, -TC10/T31N, and -Cdc42/Q61L were all prepared as describe previously (Chiang *et al.*, 2001). The dilysine point mutation TC10/KK199,200SS was prepared by polymerase chain reaction (PCR)-based site-directed mutagenesis. Deletion of the amino terminal 16 amino acids of TC10/Q75L (pKH3-ΔN-TC10/Q75L) was prepared by PCR. All other chemicals were reagent grade or the best quality commercially available. N-WASP cDNA was prepared by PCR from Quick Clone rat cDNA (CLONTECH) and was ligated into pcDNA3 with a myc-tagged sequence at the amino terminus region. N-WASP/ΔVCA cDNA was also generated by PCR and was cloned into the pcDNA3. Plasmid encoding thermoreversible folding mutant, ts045 vesicular stomatitis virus G (VSV-G) protein, fused to green fluorescent protein (GFP) at its cytoplasmic tail (VSVG-ts045-GFP) was a gift from Dr. M. McNiven (Mayo Clinic and Graduate school, Rochester, MN).

Cell Culture and Transient Transfection

3T3L1 preadipocytes were cultured in DMEM containing 25 mM glucose, 10% calf serum at 37°C in a 8% CO_2 atmosphere and induced to differentiate into adipocytes and transfected by electroporation as described previously (Min *et al.*, 1999). The cells were then allowed to adhere to tissue culture dishes for 24 h, and the adipocytes were then serum-starved for 2 h before experiments. In some experiments, the electroporated adipocytes were seeded on coverslips. Chinese hamster ovary (CHO) cells were cultured in α-minimal essential medium containing 10% fetal bovine serum and were transfected by electroporation as described previously (Yamauchi and Pessin, 1994).

Single Cell Microinjection

The microinjection and visualization of single 3T3L1 adipocytes was performed as described previously (Baumann *et al.*, 2000). Briefly, the cells were grown on coverslips and before microinjection, the medium was changed to Lebovitz's L-15 medium containing 0.1% bovine serum albumin. Differentiated 3T3L1 adipocytes were impaled using Eppendorf model 5171 micromanipulator and nuclei were injected with 50 or 200 μg/ml cDNAs in 100 mM KCl, 5 mM Na_2PO_4, pH 7.2, with a model 5246 transinjector (Eppendorf - 5 Prime, Boulder, CO). The cells were allowed to recover for 24 h and placed into a perfusion chamber maintained at 37°C and visualized by time-lapse confocal fluorescence microscopy.

Preparation of Xenopus Egg Extract

Crude *Xenopus* egg extract was prepared as described previously with slight modifications (Murray and Kirschner, 1989; Ma *et al.*, 1998; Moreau and Way, 1998). Briefly, the *X. laevis* eggs were dejellyed in 2% cysteine, pH 7.8, washed with XB solution (100 mM KCl, 50 mM sucrose, 1 mM $MgCl_2$, 0.1 mM $CaCl_2$, and 10 mM HEPES, pH 7.8, adjusted with KOH) and then washed twice with XB solution containing 5 mM EGTA and 10 μg/ml leupeptin, pepstatin A, and chymostatin. The eggs were homogenized at 4°C and centrifuged at 10,000 rpm in a SW41 rotor at 4°C for 15 min. The cytoplasmic layer was removed and 1/20 volume of energy mix (150 mM creatine phosphate, 10 mM ATP, 1 mM EGTA, and 20 mM $MgCl_2$) and 1/1000 volume of leupeptin (10 μg/ml) was added. The crude egg extract was centrifuged at 55,000 rpm in a SW60 rotor at 4°C for 1 h. The supernatant was diluted 10 times with XB solution containing 5 mM EGTA and 10 μg/ml leupeptin, pepstatin A, and chymostatin and centrifuged at 60,000 rpm in a SW60 rotor at 4°C for 1 h. The clarified cytosol was concentrated to the original volume using a Centriprep 3 concentrator (Millipore, Bedford, MA) and snap frozen in separate aliquots for storage at −80°C.

Preparation of Endosomes from CHO Cells Expressing TC10 or Cdc42

CHO cells were transfected with the TC10 and Cdc42 cDNAs by electroporation and allowed to recover for 24 h in minimal essential medium containing 10% fetal bovine serum. After 2-h serum starvation, the postnuclear supernatants containing endosome were prepared as described above.

Actin-based Motility Assay

Actin-based motility was performed in 4 μl of vesicle-free *Xenopus* egg extract containing a final concentration of 3 μM rhodamine-labeled G-actin plus 1 μl of postnuclear supernatant or 1 μl of the pellet (resuspended in 10 volume of homogenate buffer) of 3T3L1 homogenates. A 1-μl aliquot of the cell-free motility reaction was

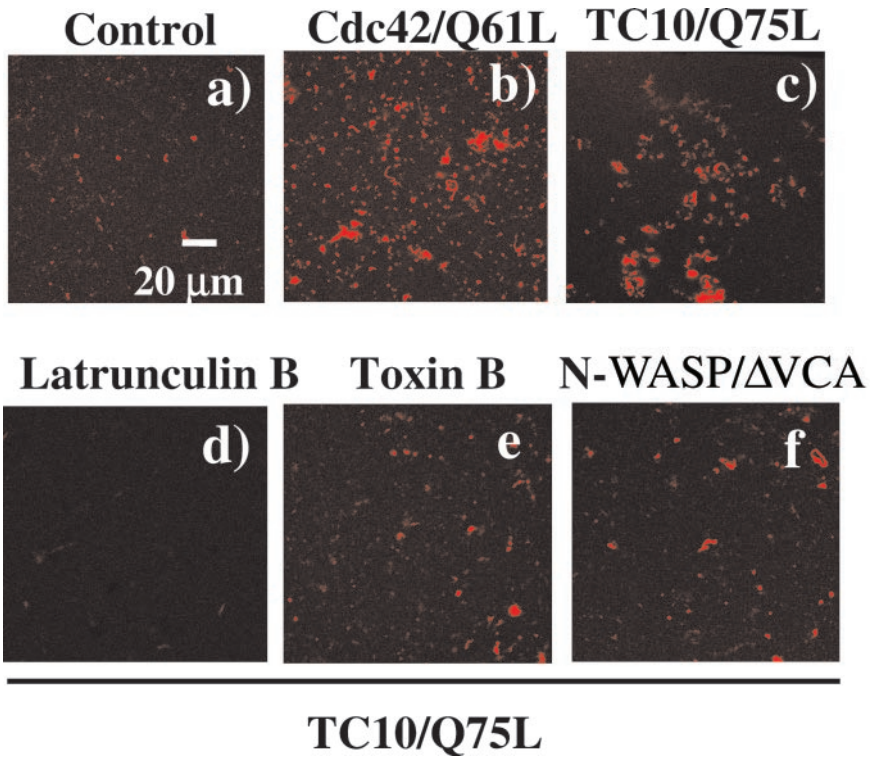

Figure 1. Activated TC10 induces actin polymerization through an N-WASP-dependent mechanism. CHO cells were transfected with either pcDNA3 (a), Cdc42/Q61L (b) or with TC10/Q75L (c–f). CHO cell extracts were prepared and mixed with *Xenopus* oocyte egg extracts plus rhodamine-actin as described under MATERIALS AND METHODS. The *Xenopus* oocyte extracts were also preincubated with 20 μM latruculin B (d), 1 μg/ml *C. difficile* toxin B (e), and 25 μg/ml N-WASP/ΔVCA dominant-interfering mutant (f) before the addition of the CHO cell extracts containing TC10/Q75L. These are representative confocal fluorescent microscopy low-magnification images taken at 10 min after the initiation of the actin polymerization assay (magnification 60×).

placed on a glass slide under a coverslip, and rhodamine images were acquired every 4 s using LSM software on PC computer equipped with a Zeiss confocal microscope. All digital images were subsequently cropped and annotated using Adobe Premiere 5.0 software (Adobe Systems, Mountain View, CA) on Macintosh computer.

Time-Lapse Confocal Fluorescence Microscopy of Living Cells Expressing Yellow Fluorescent Protein (YFP)-Actin

The YFP-actin–microinjected cells were maintained on 50-mm-diameter coverslips and were mounted in a FCS2 closed system living-cell microobservation system perfusion chamber maintained at 37°C (Bioptechs, Bulter, PA). The chamber was continuously perfused with a mixture of phenol red-free DMEM and Lebovitz's L-15 medium containing 0.1% bovine serum albumin for maintaining pH and obtaining low background fluorescence. Observations were performed on an LSM 510 inverted confocal microscope equipped with Plan-Neofluar 63×, 100× Fluar oil immersion objectives (Carl Zeiss, Thornwood, NY). All digital images were subsequently cropped and annotated using Adobe Premiere 5.0 software on Macintosh computer.

VSV-G Protein Trafficking

The VSV-G-ts045-GFP cDNA was transfected in 3T3L1 adipocytes and were maintained at 40°C for 6 h. The cells were then shifted to 32°C for 0, 10, 20, 30, 60, and 120 min and then fixed with 4% paraformaldehyde/phosphate-buffered saline. VSV-G-045ts-GFP was visualized by confocal microscopy, and the number of VSV-G-045ts-GFP–transfected cells displaying visually detectable plasma membrane rim fluorescence was counted.

RESULTS

TC10 Stimulates Actin Polymerization and Actin-based Motility In Vitro

It has been well established that activation of Cdc42, a Rho family member structurally related to TC10, can induce actin based-motility on membrane vesicles similar to that of several types of infectious bacteria such as *Listeria monocytogenes* and *Shigella flexneri* (Suzuki *et al*., 1998, 2000; Egile *et al*., 1999; Gouin *et al*., 1999; Loisel *et al*., 1999). Therefore, to determine whether TC10 can directly induce actin polymerization, we isolated vesicle-free cytosolic extracts from *Xenopus* oocytes and incubated them with rhodamine-actin plus an endosome fraction obtained from CHO cells transfected with an empty vector, or with constitutively active mutants of Cdc42 and TC10 (Figure 1). Incubation of endosomes from empty vector-transfected cells with rhodamine-actin plus vesicle-free egg extracts resulted in a very low level of in vitro actin polymerization (Figure 1a). As expected, extracts containing the constitutively active mutant Cdc42/Q61L induced a large extent of actin polymerization (Figure 1b). Similarly, addition of endosomes containing the constitutively active mutant TC10/Q75L also resulted in enhanced actin polymerization, albeit to a slightly smaller extent than did Cdc42/Q61L (Figure 1c). As controls for specificity, TC10/Q75L-induced actin polymerization was completely inhibited by treatment with latrunculin B and or the Rho family member toxin *Clostridium difficile* toxin B (Figure 1, d and e). In addition, incubation with a dominant-interfering N-WASP mutant, lacking the Arp2/3 binding region, N-WASP/ΔVCA also prevented the TC10/Q75L stimula-

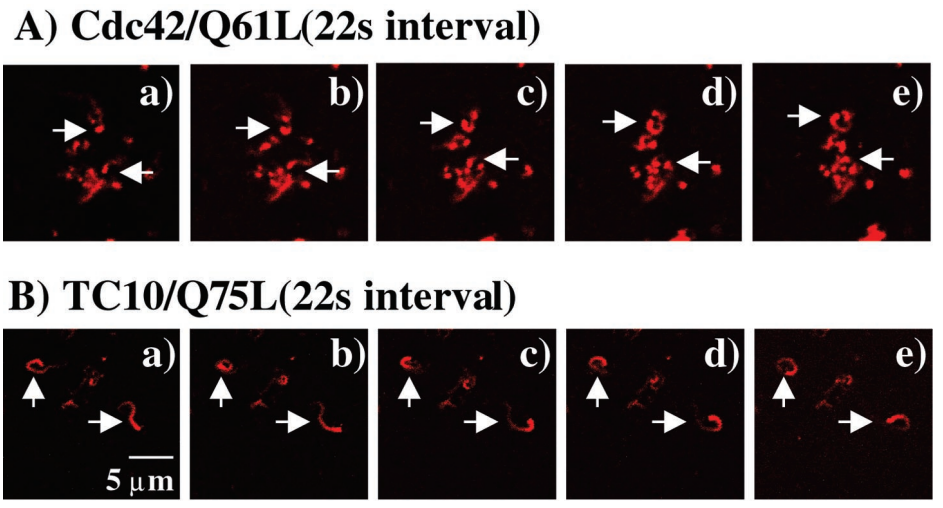

Figure 2. Time-lapse confocal microscopic observation of Cdc42/Q61L- and TC10/Q75L-induced actin comet tails. CHO cell extracts expressing Cdc42/Q61L (A) or TC10/Q75L (B) were mixed with *Xenopus* oocyte extracts plus rhodamine-actin and visualized every 22 s over a 2-min time period (a–e; magnification 100×, zoom ×2). This is a representative time-lapse image independently performed three times.

tion of actin polymerization (Figure 1f). In contrast, expression of either the dominant-interfering TC10/T31N or Cdc42/T17N mutants had no significant effect on actin polymerization (our unpublished data).

To determine whether the ability of TC10 to induce actin polymerization resulted in actin-based motility, higher resolution time-lapse images were obtained (Figure 2). As reported previously (Ma *et al.*, 1998; Moreau and Way, 1998), expression of Cdc42/Q61L resulted in the formation of long comet tails that resulted in the random propulsion of vesicles in the cell extracts (Figure 2A, a–e). TC10/Q75L was also highly effective in inducing actin comet tails as clearly visualized by the movement of polymerized rhodamine-actin in the time frames presented (Figure 2B, a–e). Together, these data demonstrate that TC10 can functionally regulate actin polymerization and comet tailing, at least in vitro, in a manner similar to that established for Cdc42.

Expression of Active TC10, but Not Cdc42, Disrupts Cortical Actin in Adipocytes

Previous studies have demonstrated that expression of constitutively active Cdc42 and TC10 mutants in fibroblasts affects actin structure, reducing actin stress fibers and in the case of TC10 strongly inducing microspike protrusions (Murphy *et al.*, 1999). However, adipocytes are round, lipid-laden cells that do not contain significant amounts of stress fibers (Omata *et al.*, 2000; Kanzaki and Pessin, 2001). Instead, these cells have a pronounced cortical actin rim beneath the plasma membrane. To examine the effect of these GTP-binding proteins on the actin cytoskeleton in adipocytes, we microinjected cDNAs encoding for a myc-epitope–tagged Cdc42/Q61L and TC10/Q75L into the cell nuclei followed by rhodamine-phalloidin labeling (Figure 3). The microinjected cells expressing the Cdc42 and TC10 proteins were identified by immunostaining with a myc monoclonal antibody (mAb) coupled with an anti-mouse IgG conjugated with fluorescein isothiocyanate (Figure 3, a and b). As typically observed, adipocytes display a strong rim of phalloidin staining in the control nonmicroinjected cells (Figure 3A, c and d). In the microinjected cells, Cdc42/Q61L was primarily distributed throughout the cytoplasm with no evidence for distinct membrane localization (Figure 3A, a). This

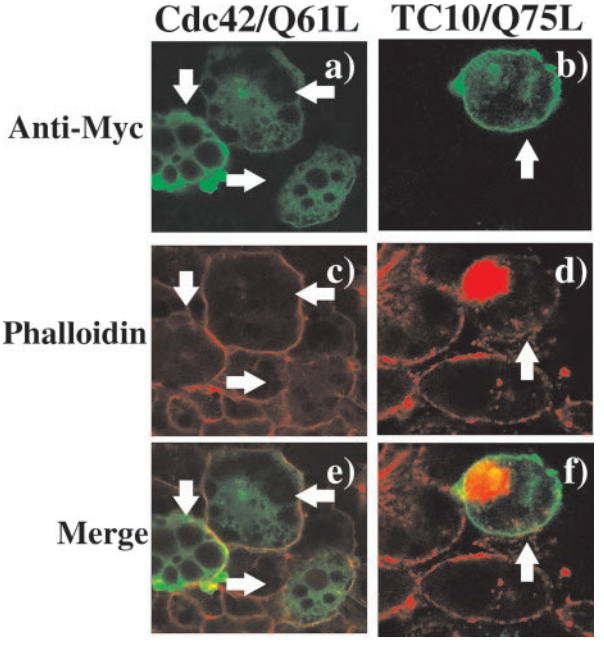

Figure 3. TC10 expression specifically disrupts cortical actin but induces actin polymerization in the perinuclear region in adipocytes. 3T3L1 adipocytes were microinjected with expression plasmids encoding for the myc-epitope–tagged Cdc42/Q61L cDNA (a, c, and e) or the TC10/Q75L cDNA (b, d, and f). The cells were allowed to recover for 24 h and then double labeled with a mAb directed against the myc-epitope tag (a and b) and with rhodamine-labeled phalloidin (c and d) as described under MATERIALS AND METHODS. The merged images are presented in e and f. This is a representative field obtained from three to five independent experiments. Quantitation of these data were obtained by counting 50–60 individual cells under each condition.

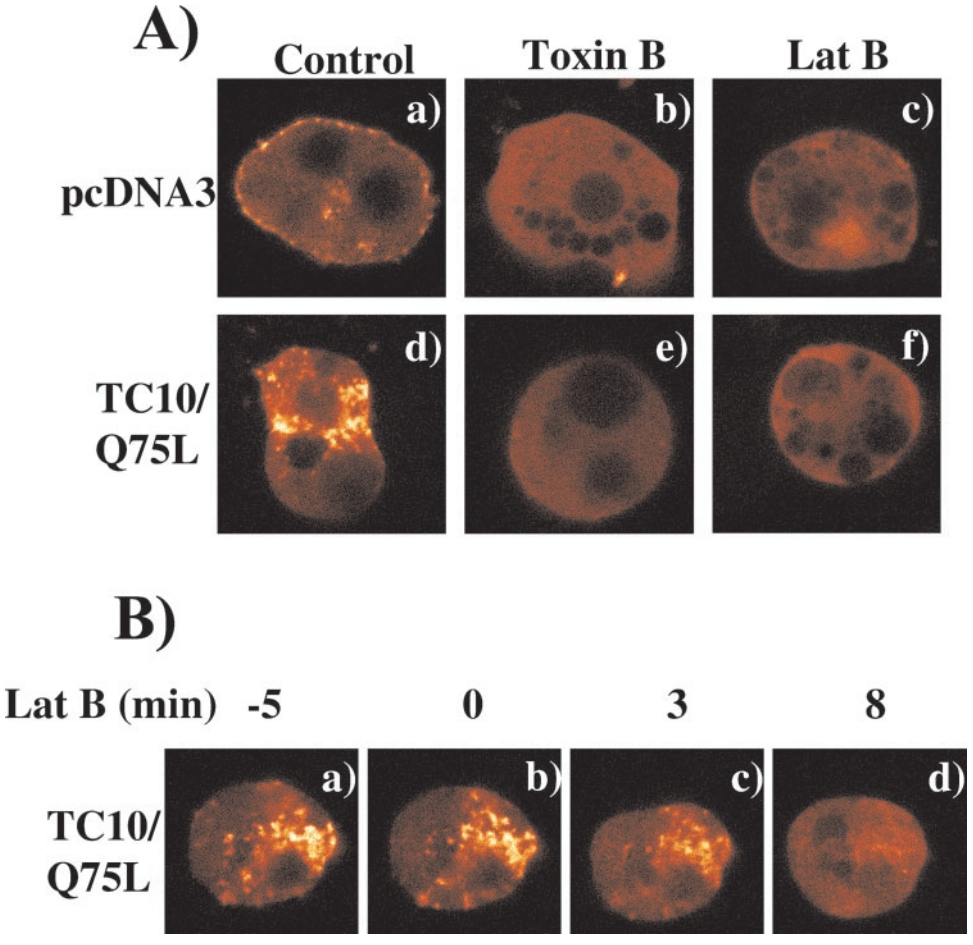

Figure 4. Expression of TC10/Q75L dirsupts cortical actin but increases perinuclear actin polymerization in adipocytes. (A) 3T3L1 adipocyte nuclei were microinjected with an expression plasmid encoding for YFP-actin plus empty vector (a–c) or TC10/Q75L (d–f) as described under MATERIALS AND METHODS. The living cells expressing YFP-actin were then continuously visualized by confocal fluorescent microscopy. The cells were also pretreated with 0.5 μg/ml *C. difficile* toxin B (b and e) or 20 μM latranculin B (c and f) followed by confocal fluorescent microscopy. The complete time-lapse image for toxin B-pretreated cell is provided in supplementary materials. (B) YFP-actin expressing cell was continuously visualized by confocal fluorescent microscopy and selected time images before and subsequent to the addition of latrunculin B (60 μM) as indicated in a–d. The complete time-lapse image is provided in supplementary materials. The time lapse images presented are representative images observed in four to seven individual cells examined under each condition.

distribution was confirmed by the detection of the Cdc42 proteins in a high-speed supernatant and not the particulate fraction after cell fractionation (our unpublished data). Importantly, expression of Cdc42/Q61L had no effect on the adipocyte cortical actin structure (Figure 3A, c and e). In contrast, TC10/Q75L was primarily localized to the plasma membrane and in the perinuclear region (Figure 3A, b). In comparison with the surrounding noninjected cells, expression of TC10/Q75L markedly reduced cortical actin labeling (Figure 3A, d). Although expression of constitutively active TC10/Q75L produced a complete disruption of cortical actin, there was a large increase in polymerized actin concentrated in the perinuclear region (Figure 3A, d and f). Quantitation of the number of cells displaying either cortical and/or perinuclear F-actin indicated that 66.1 ± 10.2% of the cells expressing of TC10/Q75L displayed a loss of cortical actin concomitant with an increased perinuclear actin. These effects on adipocyte F-actin structures were not a result of changes in cell viability because TC10/Q75L expression had no effect on GLUT1 and mannose-6-phospate receptor trafficking (Chiang *et al.*, 2001) or nuclear morphology as assessed by 4,6-diamidino-2-phenylindole staining (our unpublished data).

Activated TC10 Stimulates Perinuclear Actin Polymerization by Time-Lapse Fluorescent Microscopy In Vivo and Is Blocked by Expression of an N-WASP Mutant

The observations that activated TC10 stimulates actin comet tails in *Xenopus* oocyte extracts in vitro and F-actin accumulation in the perinuclear region in vivo, but completely disrupts cortical actin, suggest that these two actin pools are differentially regulated by TC10 in 3T3L1 adipocytes. Thus, to further investigate the dynamics of these processes in vivo, we next took advantage of an enhanced YFP-tagged β-actin (YFP-actin) to examine the actin rearrangements by time-lapse confocal microscopy (Figure 4). Previous studies have demonstrated that GFP-actin can faithfully reproduce actin polymerization and motility so long as the GFP-tagged actin was <30% native actin protein (Westphal *et al.*, 1997; Ballestrem *et al.*, 1998). Therefore, to avoid excess expression of YFP-actin, we microinjected 3T3L1 adipocyte nuclei with a relatively low amount of YFP-actin cDNA (50 μg/ml). The functional properties of the expressed YFP-actin were confirmed under these conditions because insulin characteristically stimulated membrane ruffling of the YFP-actin in predifferentiated 3T3L1 fibroblasts (our unpublished data). In the pseudocolor mode scale used to observe changes in

fluorescent intensity, expression of YFP-actin resulted in substantial background fluorescence (red), characteristic of free monomeric actin, with the more intense fluorescent areas (white) indicative of polymerized actin. In the control cells comicroinjected with empty vector, there was a low level of polymerized actin present beneath the plasma membrane (cortical actin) with some punctate accumulation in the perinuclear region (Figure 4A, a). Treatment with either latrunculin B or the Rho family-specific toxin *C. difficile* toxin B resulted in a complete disruption of both cortical and perinuclear polymerized actin (Figure 4A, b and c). As previously observed using rhodamine-phalloidin staining, expression of TC10/Q75L resulted in a marked increase in perinuclear actin polymerization with a concomitant disruption of cortical actin (Figure 4A, d). Similarly, treatment of these cells with either toxin B or latrunculin B completely dispersed all the intracellular polymerized actin (Figure 4A, e and f).

Latrunculin specifically binds monomeric actin and prevents the incorporation of monomeric actin into growing actin chains (Coue *et al.*, 1987; Morton *et al.*, 2000). Importantly, latrunculin does not sever F-actin and thereby indirectly results in actin depolymerization by reducing the functional actin monomer concentration (Coue *et al.*, 1987). We therefore took advantage of latrunculin B to determine whether the perinuclear actin was capable of undergoing continuous remodeling (Figure 4B). As expected, expression of TC10/Q75L induced perinuclear actin that was clearly detected by the polymerization of coexpressed YFP-actin (Figure 4B, a). Addition of latrunculin B resulted in a time-dependent decrease in the amount of perinuclear F-actin (Figure 4B, b–d). These data demonstrate that activated TC10 stimulates continuous perinuclear actin remodeling but completely disrupts cortical actin in adipocytes.

We next examined the functional role of N-WASP in the TC10/Q75L-induced perinuclear actin polymerization in vivo (Figure 5). Expression of YFP-actin in control cells demonstrated the presence of cortical actin juxtaposed to the plasma membrane with a small amount of perinuclear polymerized actin (Figure 5a). Expression of the dominant-interfering N-WASP mutant (N-WASP/ΔVCA) had no effect on cortical actin as assessed by YFP-actin (Figure 5b). Consistent with our previous data, expression of TC10/Q75L dramatically increased the extent of perinuclear polymerized actin (Figure 5c). This actin was still able to undergo dynamic remodeling as observed by changes in actin polymerization after insulin stimulation (our unpublished data). In contrast, coexpression of N-WASP/ΔVCA markedly reduced the extent of polymerized actin in the perinuclear region (Figure 5d). The inhibitory effect of N-WASP/ΔVCA on TC10/Q75L-induced actin polymerization is easily visualized in the time-lapse video presented in the supplementary information. Quantitation of the YFP-actin fluorescent intensity indicated that expression of N-WASP/ΔVCA reduced the extent of TC10/Q75L-induced perinuclear actin polymerization by 61.7 ± 0.6%. Importantly, the N-WASP/ΔVCA inhibition of TC10/Q75L-induced perinuclear actin polymerization occurred without any change in the levels of TC10Q/75L protein expression (our unpublished data).

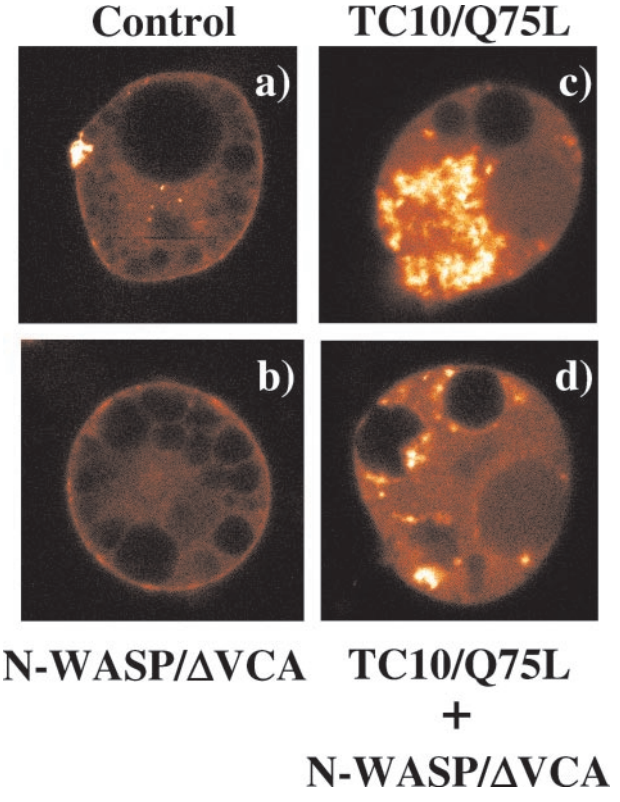

Figure 5. TC10/Q75L expression induces perinuclear actin polymerization that is inhibited by a dominant-interfering N-WASP mutant. 3T3L1 nuclei were microinjected with expression plasmids encoding for YFP-actin plus either the empty vector (a), N-WASP/ΔVCA (b), TC10/Q75L (c), or N-WASP/ΔVCA plus TC10/Q75L (d). The cells were allowed to recover for 24 h and then visualized by time-lapse confocal fluorescent microscopy. These are individual representative YFP-actin time-lapse fluorescent images observed in four to seven independent cells examined.

Inhibition of Cortical Actin but Not Perinuclear Actin Is Specific for the Amino Terminal Extension of TC10

Having established that TC10/Q75L has the capability of inducing actin polymerization in vitro and perinuclear actin in vivo, we next addressed the basis for the disruption of cortical actin by TC10/Q75L. Sequence comparison between human TC10 and other Rho family members of small GTP-binding proteins indicated that TC10 has a unique amino terminal extension. To assess the potential role of this 16-amino acid extension, we compared the effect of TC10/Q75L and an amino terminal deletion (ΔN-TC10/Q75L) on F-actin structure in 3T3L1 adipocytes (Figure 6). As observed previously, the expressed TC10/Q75L protein was localized to both the plasma membrane and the perinuclear region (Figure 6a). As expected, the cells expressing TC10/Q75L displayed a strong induction of perinuclear actin polymerization but disrupted cortical actin (Figure 6, b and c). As expected, the expressed ΔN-TC10/Q75L protein resulted in a similar intracellular distribution as TC10/Q75L and markedly stimulated perinuclear actin polymerization (Figure 6,

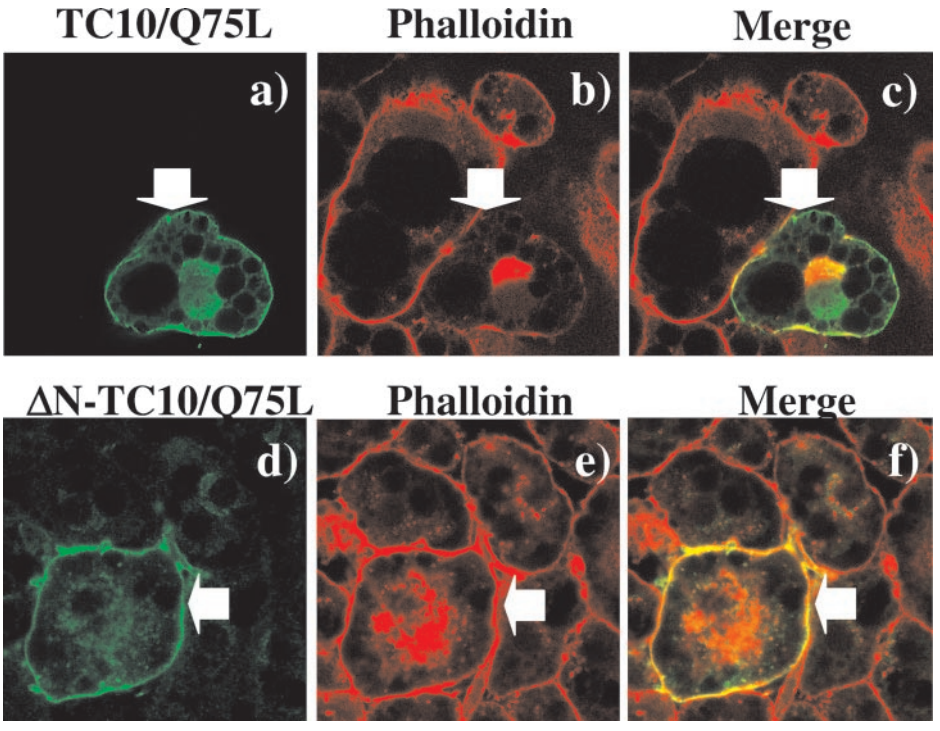

Figure 6. Amino terminal domain of TC10/Q75L is responsible for the loss of adipocyte cortical actin. 3T3L1 adipocyte nuclei were microinjected with expression plasmids encoding for TC10/Q75L (a–c) and ΔN-TC10/Q75L (d–f). The cells were allowed to recovery for 24 h and then double labeled with a mAb directed against the myc-epitope tag (a and d) and with rhodamine-labeled phalloidin (b and e) as described under MATERIALS AND METHODS. The merged images are presented in c and f. This is a representative field obtained from three independent experiments. In each experimental condition a total of 53 to 77 individual cells were scored for the presence of cortical actin.

d–f). However, in contrast to TC10/Q75L, adipocyte cortical actin was completely resistant to ΔN-TC10/Q75L expression (Figure 6, e and f). Quantitation of these data demonstrated that compared with TC10/Q75L (66.1 ± 10.2%) only 15.7 ± 3.7% of the cells expressing DN-TC10/Q75L had a loss of cortical actin. Together, these data demonstrate that the amino terminal domain of TC10 is required for the disruption of cortical actin, whereas the effector binding domains mediate F-actin polymerization.

Perinuclear Actin Polymerization Occurs in Golgi Region and Modulates Cargo Vesicle Transport

The major perinuclear membrane compartments in adipocytes are the Golgi apparatus and endosome compartments. To assess whether the large TC10/Q75L-stimulated increase in perinuclear actin occurred in the Golgi, we examined the colocalization of TC10/Q75L and the *cis*-Golgi marker p115 with phalloidin-labeled actin (Figure 7). As previously observed, TC10/Q75L was localized to the plasma membrane but was also detectable in various endomembrane compartments, including the perinuclear region (Figure 7, a and e). Phalloidin staining demonstrated the expected large increase in perinuclear actin in cells expressing TC10/Q75L concomitant with the disruption of cortical actin labeling (Figure 7, b and f). The Golgi membrane marker p115 was also predominantly confined to the perinuclear region (Figure 7, c and g). Furthermore, the perinuclear F-actin colocalized with p115 and TC10/Q75L in a pattern analogous to actin comet tails. It should also be noted that in the presence of TC10/Q75L Golgi appears more diffuse and extended than that observed in control cells (Figure 7g). Thus, these data demonstrate that TC10 can affect Golgi structure and importantly the organization and regulation of Golgi actin.

Previous studies have suggested that Golgi actin plays a regulatory role in membrane vesicle transport (Godi *et al.*, 1998; Hirschberg *et al.*, 1998; De Matteis and Morrow, 2000; Fucini *et al.*, 2000, 2002; Valderrama *et al.*, 2000, 2001). To determine whether perinuclear actin plays a regulatory role in endomembrane trafficking, we took advantage of the temperature-sensitive VSV-G protein mutant ts045. Incubation of cells at the nonpermissive temperature 40°C prevents VSV-G protein exit from the endoplasmic reticulum (Presley *et al.*, 1997; Nehls *et al.*, 2000). However, temperature shift to 32°C allows for the transport of VSV-G protein to the Golgi, subsequent entry to the secretory membrane system and accumulation at the plasma membrane. As expected, adipocytes maintained at 40°C displayed a diffuse membrane distribution of VSV-G protein characteristic of the endoplasmic recticulum (Figure 8A, a, c, e, and g). After temperature shift to 32°C for 60 min, VSV-G protein was able to accumulate at the plasma membrane (Figure 8A, b). In contrast, adipocytes coexpressing TC10/Q75L had a markedly reduced extent of VSV-G trafficking to the plasma membrane (Figure 8A, c and d). In comparison, expression of a dominant-interfering TC10 mutant (TC10/T31N) that depolymerizes perinuclear actin had a partially inhibitory effect (Kanzaki and Pessin, 2001) (Figure 8A, e and f). Furthermore, expression of N-WASP/ΔVCA also resulted in a reduced rate of VSV-G protein transport to the plasma membrane (Figure 8A, g and h). Quantitation of these data indicate that the accumulation of VSV-G protein at the cell surface occurred with an approximate 30-min half-time and near complete plasma membrane localization by 120 min (Figure 7B, solid circles). Expression of TC10/Q75L delayed and reduced the rate of VSV-G protein transport to the plasma membrane (Figure 8B, open squares). Similarly, depolymer-

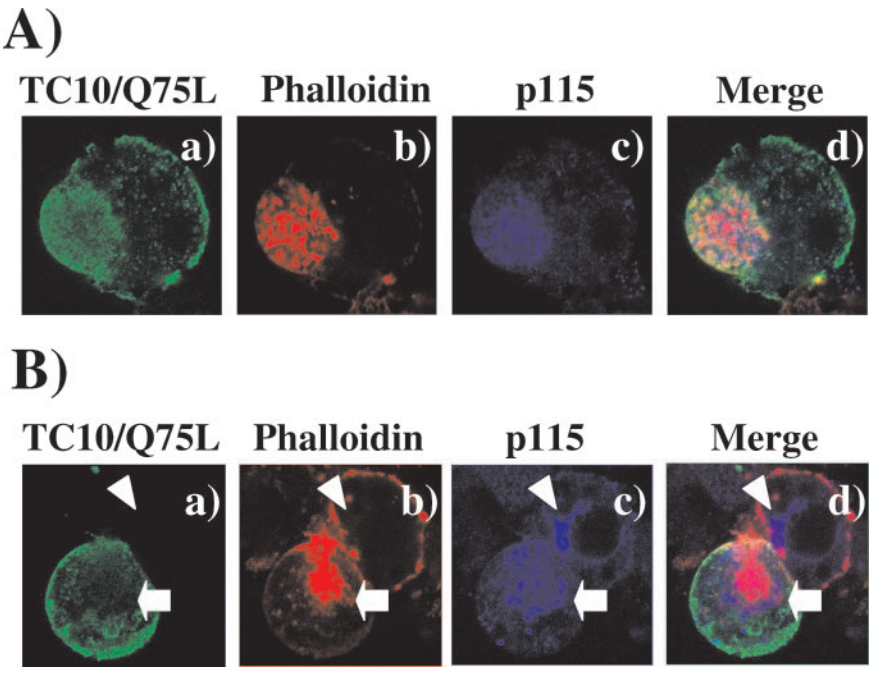

Figure 7. TC10/Q75L induces massive actin polymerization in the Golgi membrane region of adipocytes. 3T3L1 adipocytes were electroporated with expression plasmid encoding for the myc-tagged TC10/Q75L and the cells were allowed to recover for 24 h. The cells were then fixed and triple labeled with a rabbit polyclonal antibody directed against the myc-epitope tag (a and e), rhodamine-labeled phalloidin (b and f), and a mouse mAb directed against the p115 (c and g) as described under MATERIALS AND METHODS. The merged images are presented in d and h. These are representative fields obtained from three independent experiments.

ization of Golgi actin by TC10/T31N and N-WASP/ΔVCA also resulted in a reduced rate of general membrane transport out of the Golgi (Figure 8B; TC10/T31N, solid squares, and N-WASP/ΔVCA, open circles). These data demonstrate that disruption of the normal Golgi actin architecture and its proper remodeling correlate with changes in secretory membrane protein transport.

TC10 Directly Interacts with COPI Coat Proteins

Recent studies have suggested that in fibroblasts Cdc42 can be recruited to the Golgi through interactions with coatomer (Fucini *et al.*, 2002; Wu *et al.*, 2000). In addition, Cdc42 was observed to regulate Golgi vesicle transport (Wu *et al.*, 2000; Musch *et al.*, 2001). Because TC10 also mediates Golgi actin assembly and modulates Golgi vesicle transport, we examined the interaction of TC10 with coatomer (Figure 9). As reported previously, expression of the constitutively active Cdc42 mutant (Cdc42/Q61L) resulted in the coimmunoprecipitation with coatomer as assessed by the appearance of the β-COP subunit (Figure 9A, lanes 1 and 3). In parallel, expression of constitutively active TC10/Q75L also resulted in a similar extent of β-COP coimmunoprecipitation (Figure 9A, lane 2). Although TC10/WT was fully capable of coimmunoprecipitating β-COP, this interaction was not detected with the dominant-negative TC10/T31N mutant (Figure 9A, lanes 4–6). The interaction of Cdc42 with coatomer is thought to be through a direct binding interaction of a carboxyl terminal dilysine motif with the γ-COP subunit (Wu *et al.*, 2000). Immunoprecipitation of expressed TC10/WT and TC10/Q75L but not TC10/T31N resulted in the coimmunoprecipitation of γ-COP (Figure 9B, lanes 1–4). Furthermore, expression of the dilysine mutant (TC10/KK199,200SS) had a near complete loss of γ-COP binding (Figure 9B, lane 5). Taken together, these data are consistent with TC10 inducing perinuclear actin polymerization and regulating Golgi transport vesicles through its bifunctional interactions between N-WASP and coatomer.

DISCUSSION

Recent studies have documented that Rho family GTP-binding proteins can function as molecular switches linking cell surface receptors and other extracellular cues to the regulation of actin dynamics (Hall, 1998). In motile cells, actin cytoskeleton-membrane interactions drive the formation and retraction of stress fibers, lamellipodia, and filopodia principally controlled by Rho, Rac, and Cdc42, respectively (Ridley and Hall, 1992; Ridley *et al.*, 1992; Kozma *et al.*, 1995, 1996; Nobes and Hall, 1995). More recently Cdc42, a protein structurally related to TC10, has been established to induce actin-based motility on membrane vesicles similar to that of several types of infectious bacteria such as *L. monocytogenes* and *S. flexneri* (Suzuki *et al.*, 1998, 2000; Egile *et al.*, 1999; Gouin *et al.*, 1999; Loisel *et al.*, 1999; Taunton *et al.*, 2000). Unlike other Rho family member proteins that act predominantly through the bundling of preexisting actin structures, Cdc42 stimulates de novo actin polymerization, including actin comet tails, a process mediated by N-WASP, WAVE, and actin-related protein Arp2/3 (Machesky and Insall, 1999). Consistent with the high degree of structural similarity between Cdc42 and TC10, by using *Xenopus* oocyte extracts as the source for actin and actin cofactors, we have observed that TC10 can potently induce actin comet tails that are inhibited by a dominant-interfering N-WASP mutant (N-WASP/ΔVCA) in a manner analogous to that established for Cdc42 in vitro. These data demonstrate that TC10 has the capacity to induce actin polymerization and actin-based motility in vitro.

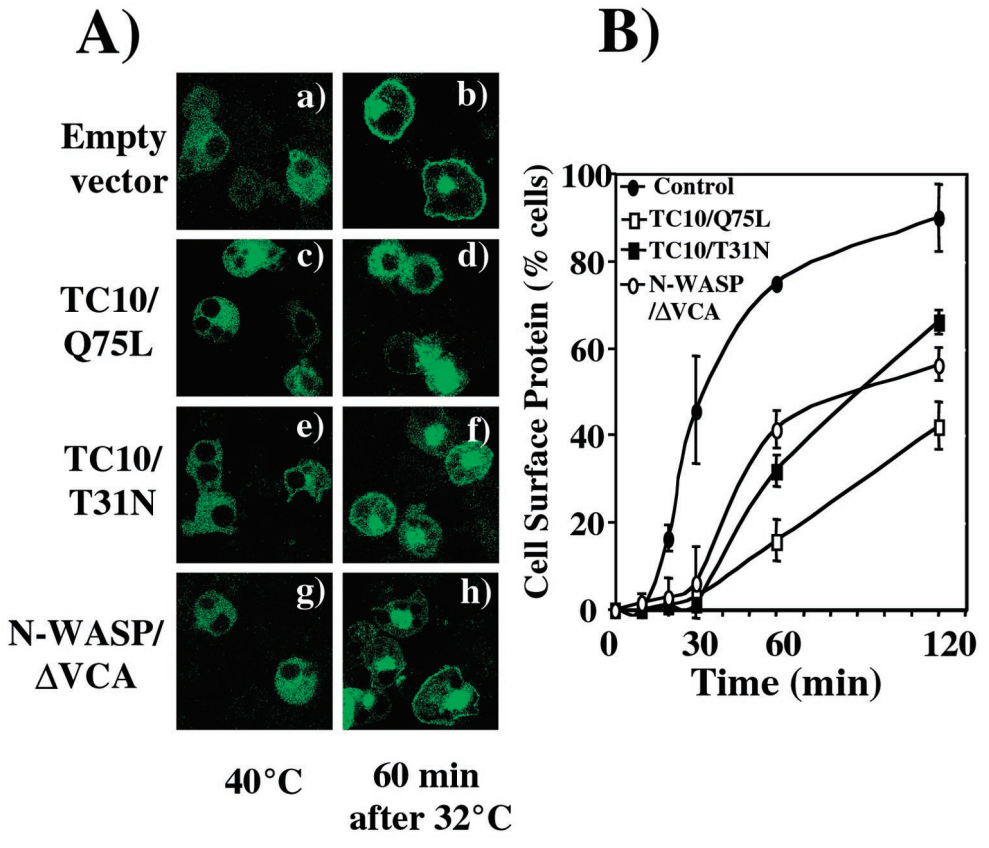

Figure 8. Derangement of perinuclear actin inhibits VSV-G protein trafficking. (A) 3T3L1 adipocytes were coelectroporated with expression plasmids encoding for theVSV-G-ts045-GFP with either the empty vector (a and b) or expression plasmids encoding for TC10/Q75L (c and d), TC10/T31N (e and f), or N-WASP/ΔVCA (g and h) cDNA. The cells were incubated for 6 h at 40°C and then shifted to 32°C for 60 min. The cells were fixed and VSV-G-ts045-GFP was visualized by confocal microscopy. (B) The number of VSV-G-ts045-GFP-expressing cells displaying visually detectable plasma membrane fluorescence was counted from seven different fields (75–150 transfected cells/condition). This graph shows a result from two independent experiments from empty vector cotransfected adipocytes (●) or adipocytes coexpressing TC10/Q75L (□), TC10/T31N (■), or N-WASP/ΔVCA (○) cDNAs.

However, the regulation of actin polymerization by TC10 in intact adipocytes seems to be significantly different than that observed in vitro. For example, we could not detect the formation of long actin comet tails by using YFP-actin expression in intact cells. This is probably due to poorer resolution of actin polymerization in adipocytes, resulting from the presence of the large lipid droplets and/or the likelihood that the length of the comet tails in vivo is below the level of sensitivity. Alternatively, it is also possible that the actin comet tails might be short-lived in intact cells and therefore difficult to observe.

In any case, model fibroblast tissue culture systems have been used to examine the functional roles of the Rho family GTP-binding proteins. However, the data obtained in fibroblast cell lines cannot be extrapolated to adipocytes. Unlike fibroblasts, fully differentiated adipocytes are rounded lipid-laden cells that do not contain significant amounts of stress fibers, lamellipodia, or filopodia. Instead, the majority of the polymerized actin seems to concentrate in the perinuclear region (Golgi) and around the inner face of the plasma membrane (cortical actin). The data presented in this manuscript demonstrate that Cdc42 does not play a significant role in the regulation of F-actin structures in differentiated adipocytes. This is consistent with our previous studies demonstrating that insulin activates TC10 but not Cdc42 in adipocytes (Chiang *et al.*, 2001). In addition to the apparent adipocyte specificity, TC10 clearly differentially regulates two distinct compartmentalized actin populations that depend on TC10 localization. Expression of TC10/Q75L completely disrupted the adipocyte cortical actin, whereas the perinuclear actin underwent massive polymerization. Importantly, expression of N-WASP/ΔVCA had no significant effect on cortical actin. In contrast, N-WASP/ΔVCA inhibited TC10/Q75L induced perinuclear actin polymerization. Because the N-WASP/ΔVCA mutant is thought to prevent endogenous effector binding (i.e., N-WASP) to both TC10 and Cdc42, this would prevent the recruitment of the Arp2/3 complex to growing actin chains and thereby inhibit N-WASP–dependent actin polymerization.

How then is it possible that constitutively active TC10/Q75L stimulates perinuclear actin polymerization yet disrupts cortical actin? We hypothesized that TC10 might have two opposing functional domains, the effector domain that stimulates actin polymerization and another domain that inhibits actin polymerization. Inspection of the human TC10 sequences revealed the presence of a unique amino terminal extension that is not present in other small GTP-binding proteins. Consistent with the prediction that this 16-amino acid sequence provides a negative function, expression of an amino terminal deletion of TC10/Q75L had no significant effect on cortical actin structure but was still fully capable of inducing perinuclear actin polymerization. This finding is also consistent with the effect of N-WASP/ΔVCA expression, which blocks perinuclear actin polymerization by inhibiting the TC10 effector binding domain. Thus, these data support the presence of two distinct mechanisms being responsible for the control of cortical and perinuclear actin polymerization in adipocytes.

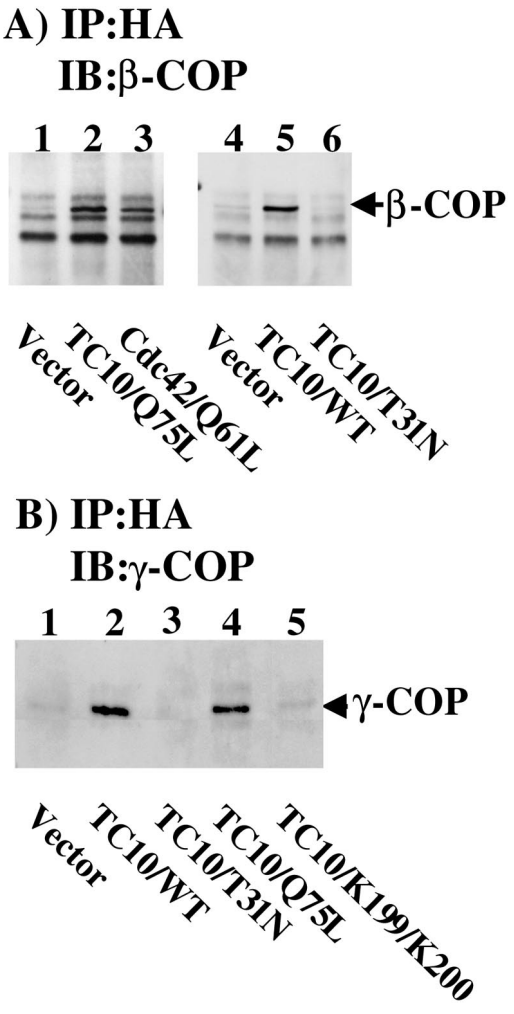

Figure 9. TC10 interacts with coatomer through a carboxyl-terminal dilysine motif. (A) 3T3L1 adipocytes were electroporated with empty vector (lane 1) or expression plasmids encoding for the hemagglutinin-epitope–tagged TC10/Q75L (lane 2), Cdc42/Q61L (lane 3), empty vector (lane 4), TC10/WT (lane 5), or TC10/T31N (lane 6). The cells were allowed to recover for 24 h and then immunoprecipitated with the hemagglutinin antibody and immunoblotted with a β-COP antibody as described under MATERIALS AND METHODS. (B) 3T3L1 adipocytes were electroporated with empty vector (lane 1) or expression plasmids encoding for the hemigglutinin-epitope–tagged TC10/WT (lane 2), TC10/T31N (lane 3), TC10/Q75L (lane 4), or TC10/KK199,200SS (lane 5). The cells were allowed to recover for 24 h and then immunoprecipitated with the hemigglutinin antibody and immunoblotted with a γ-COP antibody as described under MATERIALS AND METHODS. These are representative immunoprecipitations independently performed three times.

Recent studies have directly implicated Cdc42 and actin in membrane trafficking through the Golgi. For example, actin has been observed on Golgi-derived membrane vesicles and can assemble on Golgi membranes in vitro (Musch *et al.*, 1997; Godi *et al.*, 1998; Heimann *et al.*, 1999; Fucini *et al.*, 2000; Valderrama *et al.*, 2000). Cdc42 also seems to associate with Golgi-membranes and to induce actin polymerization through the engagement of N-WASP (Fucini *et al.*, 2002; McCallum *et al.*, 1998; Moreau *et al.*, 2000; Wu *et al.*, 2000). In this regard, Cdc42 has recently been found to differentially regulate *trans*-Golgi network exit of proteins destined for the apical or basolateral membranes of polarized epithelial cells (Musch *et al.*, 2001). Although we could not detect any consequence of Cdc42 expression in adipocytes, these recent observations are consistent with the function of TC10 in this cell system.

Cdc42 can also directly bind γ-COP in a GTP-dependent manner through a carboxyl-terminal dilysine motif (Wu *et al.*, 2000). Because γ-COP exists in a tight coatomer complex, this also results in the coimmunoprecipitation of the other coat proteins, including β-COP. Similar to Cdc42, the carboxyl-terminal domain of TC10 also contains a dilysine motif and coimmunoprecipitates both β- and γ-COP in a GTP-dependent manner. Furthermore, mutation of these lysine residues prevents the interaction of TC10 with coatomer.

Several studies have also implicated a role for actin in the regulation of Golgi membrane transport and vesicle sorting decisions. For example, treatment of cells with cytochalasin B to sever F-actin decreased the rate of Golgi protein transport (Hirschberg *et al.*, 1998; Valderrama *et al.*, 2001). Golgi-derived COPI-coated vesicles were found to directly associate with polymerized actin necessary for retrograde transport to the endoplasmic recticulum (Valderrama *et al.*, 2000, 2001). The ability of TC10 to bind COPI protein subunits and to induce massive Golgi membrane actin polymerization strongly suggests that Cdc42 and TC10 function in a similar manner in the control of perinuclear actin dynamics. However, these functions are cell context dependent with Cdc42 functioning in fibroblasts and polarized epithelial cells, whereas TC10 plays a more restrictive role in adipocytes. This would be consistent with TC10 directing more specialized vesicle trafficking in adipocyte due to its specific targeting to lipid raft microdomains (Watson *et al.*, 2001).

Our data also demonstrate that Golgi actin dynamics play an important regulatory role in adipocyte membrane transport. Expression of the constitutively active TC10/Q75L mutant resulted in a marked decrease in VSV-G protein trafficking concomitant with massive actin polymerization in the Golgi complex. However, disruption of Golgi actin with TC10/T31N also impaired VSV-G protein transport through the Golgi complex. Similarly, expression of N-WASP/ΔVCA also resulted in a decrease in VSV-G protein transport to the plasma membrane. This duality of actin function is also similar to the depolymerization of actin by latrunculin B/cytochalasin D vs. enhanced actin polymerization by Cdc42 to alter Golgi membrane transport (Hirschberg *et al.*, 1998; Wu *et al.*, 2000; Musch *et al.*, 2001; Valderrama *et al.*, 2001). This apparent discordance can be reconciled based upon reports examining dense core granule secretion. These studies have demonstrated that actin can act as both a positive and negative regulator depending upon the degree of actin polymerization. For example, it has been suggested that actin can function as a physical barrier to vesicle docking based upon its transient depolymerization during exocytosis such that secretion preferentially occurs at sites where the actin cortex is relatively thin (Bernstein and Bamburg, 1989; Vitale *et al.*, 1991, 1995; Norman *et al.*, 1996; Carbajal and Vitale, 1997). Furthermore, in some cases disruption of the actin cytoskeleton markedly potentiates agonist-stimulated secretion

(Lelkes *et al*., 1986; Sontag *et al*., 1988; Matter *et al*., 1989; Muallem *et al*., 1995). In contrast however, in many cell systems depletion of F-actin structures either by sequestering actin monomers or by stimulation of actin severing does not stimulate exocytosis but rather results in an inhibition of agonist-induced secretion (Morita *et al*., 1988; O'Konski and Pandol, 1990; O'Konski and Pandol, 1993; Li *et al*., 1994). These findings are consistent with a requirement for active actin remodeling during the transport process rather than a requirement for static actin structures. Thus, taken together our data demonstrate that TC10 can function in adipocytes as an important regulator of perinuclear actin polymerization that is necessary for efficient membrane protein trafficking. Therefore, alterations in this balance either by completely disrupting perinuclear actin or by excess polymerization negatively affect this process.

Consistent with these observations, we and others have observed that the balance between actin polymerization/depolymerization is also critical in the regulation of GLUT4 translocation. For example, various agents that either disrupt filamentous actin structures or stabilize F-actin effectively inhibit insulin-stimulated GLUT4 trafficking events (Tsakiridis *et al*., 1994; Wang *et al*., 1998; Kanzaki and Pessin, 2001; Tong *et al*., 2001). Similarly, overexpression of TC10/Q75L that induces massive perinuclear actin polymerization but completely disrupts cortical actin also inhibits insulin-stimulated GLUT4 trafficking in a manner identical to TC10/T31N (Kanzaki and Pessin, 2001). Furthermore, we recently demonstrated the formation of actin comet tails on GLUT4-containing endosomes that are blocked in the presence of the N-WASPΔVCA (Kanzaki *et al*., 2001). Together, these data strongly support a model in which different populations of F-actin function in distinct aspects of regulated and constitutive membrane trafficking events. Further studies are now needed to determine the precise molecular events responsible for differential regulation of cortical and perinuclear actin by TC10.

ACKNOWLEDGMENTS

This work was support by grants DK-25295 and DK-59291 from the National Institutes of Health (to J.E.P.) and from the American Cancer Society (to M.S.).

REFERENCES

Ballestrem, C., Wehrle-Haller, B., and Imhof, B.A. (1998). Actin dynamics in living mammalian cells. J. Cell Sci. *111*, 1649–1658.

Baumann, C.A., Ribon, V., Kanzaki, M., Thurmond, D.C., Mora, S., Shigematsu, S., Bickel, P.E., Pessin, J.E., and Saltiel, A.R. (2000). CAP defines a second signaling pathway required for insulin-stimulated glucose transport. Nature *407*, 202–207.

Bernstein, B.W., and Bamburg, J.R. (1989). Cycling of actin assembly in synaptosomes and neurotransmitter release. Neuron *3*, 257–265.

Carbajal, M.E., and Vitale, M.L. (1997). The cortical actin cytoskeleton of lactotropes as an intracellular target for the control of prolactin secretion. Endocrinology *138*, 5374–5384.

Chiang, S.-H., Baumann, C.A., Kanzaki, M., Watson, R.T., Thurmond, D.C., Macara, I.G., Pessin, J.E., and Saltiel, A.R. (2001). Insulin-stimulated GLUT4 translocation requires the CAP-dependent activation of the small GTP binding protein TC10. Nature *410*, 944–948.

Coghlan, M.P., Chou, M.M., and Carpenter, C.L. (2000). Atypical protein kinases Clambda and -zeta associate with the GTP-binding protein Cdc42 and mediate stress fiber loss. Mol. Cell. Biol. *20*, 2880–2889.

Coue, M., Brenner, S.L., Spector, I., and Korn, E.D. (1987). Inhibition of actin polymerization by latrunculin A. FEBS Lett. *213*, 316–318.

De Matteis, M.A., and Morrow, J.S. (2000). Spectrin tethers and mesh in the biosynthetic pathway. J. Cell Sci. *113*, 2331–2343.

Egile, C., Loisel, T.P., Laurent, V., Li, R., Pantaloni, D., Sansonetti, P.J., and Carlier, M.F. (1999). Activation of the CDC42 effector N-WASP by the *Shigella flexneri* IcsA protein promotes actin nucleation by Arp2/3 complex and bacterial actin-based motility. J. Cell Biol. *146*, 1319–1332.

Fucini, R.V., Chen, J.-L., Sharma, C., Kessels, M.M., and Stamnes, M. (2002). Golgi vesicle proteins are linked to the assembly of an actin complex defined by mAbp1. Mol. Biol. Cell *13*, 621–631.

Fucini, R.V., Navarrete, A., Vadakkan, C., Lacomis, L., Erdjument-Bromage, H., Tempst, P., and Stamnes, M. (2000). Activated ADP-ribosylation factor assembles distinct pools of actin on Golgi membranes. J. Biol. Chem. *275*, 18824–18829.

Godi, A., *et al*. (1998). ADP ribosylation factor regulates spectrin binding to the Golgi complex. Proc. Natl. Acad. Sci. USA *95*, 8607–8612.

Gouin, E., Gantelet, H., Egile, C., Lasa, I., Ohayon, H., Villiers, V., Gounon, P., Sansonetti, P.J., and Cossart, P. (1999). A comparative study of the actin-based motilities of the pathogenic bacteria *Listeria monocytogenes*, *Shigella flexneri* and *Rickettsia conorii*. J. Cell Sci. *112*, 1697–1708.

Hall, A. (1998). Rho GTPases and the actin cytoskeleton. Science *279*, 509–514.

Heimann, K., Percival, J.M., Weinberger, R., Gunning, P., and Stow, J.L. (1999). Specific isoforms of actin-binding proteins on distinct populations of Golgi-derived vesicles. J. Biol. Chem. *274*, 10743–10750.

Hirschberg, K., Miller, C.M. Ellenberg, J., Presley, J.F., Siggia, E.D., Phair, R.D., and Lippincott-Schwartz, J. (1998). Kinetic analysis of secretory protein traffic and characterization of Golgi to plasma membrane transport intermediates in living cells. J. Cell Biol. *143*, 1485–1503.

Imagawa, M., Tsuchiya, T., and Nishihara, T. (1999). Identification of inducible genes at the early stage of adipocyte differentiation of 3T3–L1 cells. Biochem. Biophys. Res. Commun. *254*, 299–305.

Joberty, G., Perlungher, R.R., and Macara, I.G. (1999). The Borgs, a new family of Cdc42 and TC10 GTPase-interacting proteins. Mol. Cell. Biol. *19*, 6585–6597.

Joberty, G., Petersen, C., Gao, L., and Macara, I.G. (2000). The cell-polarity protein Par6 links Par3 and atypical protein kinase C to Cdc42. Nat. Cell Biol. *2*, 531–539.

Kanzaki, M., and Pessin, J.E. (2001). Insulin-stimulated GLUT4 translocation in adipocytes is dependent upon cortical actin remodeling. J. Biol. Chem. *276*, 42436–42434.

Kanzaki, M., Watson, R.T., Khan, A.H. and Pessin, J.E. (2001). Insulin-stimulates actin comet tails on intracellular GLUT4-containing compartments in differentiated 3T3L1 adipocytes. J. Biol. Chem. *276*, 49331–49336.

Kozma, R., Ahmed, S., Best, A., and Lim, L. (1995). The Ras-related protein Cdc42Hs and bradykinin promote formation of peripheral actin microspikes and filopodia in Swiss 3T3 fibroblasts. Mol. Cell. Biol. *15*, 1942–1952.

Kozma, R., Ahmed, S., Best, A., and Lim, L. (1996). The GTPase-activating protein n-chimaerin cooperates with Rac1 and Cdc42Hs

to induce the formation of lamellipodia and filopodia. Mol. Cell. Biol. *16*, 5069–5080.

Lelkes, P.I., Friedman, J.E., Rosenheck, K., and Oplatka, A. (1986). Destabilization of actin filaments as a requirement for the secretion of catecholamines from permeabilized chromaffin cells. FEBS Lett. *208*, 357–363.

Li, G., Rungger-Brandle, E., Just, I., Jonas, J.C., Aktories, K., and Wollheim, C.B. (1994). Effect of disruption of actin filaments by *Clostridium botulinum* C2 toxin on insulin secretion in HIT-T15 cells and pancreatic islets. Mol. Biol. Cell *5*, 1199–1213.

Loisel, T.P., Boujemaa, R., Pantaloni, D., and Carlier, M.F. (1999). Reconstitution of actin-based motility of *Listeria* and *Shigella* using pure proteins. Nature *401*, 613–616.

Ma, L., Rohatgi, R., and Kirschner, M.W. (1998). The Arp2/3 complex mediates actin polymerization induced by the small GTP-binding protein Cdc42. Proc. Natl. Acad. Sci. USA *95*, 15362–15367.

Machesky, L.M., and Insall, R.H. (1999). Signaling to actin dynamics. J. Cell Biol. *146*, 267–272.

Matter, K., Dreyer, F., and Aktories, K. (1989). Actin involvement in exocytosis from PC12 cells: studies on the influence of botulinum C2 toxin on stimulated noradrenaline release. J. Neurochem. *52*, 370–376.

McCallum, S.J., Erickson, J.W., and Cerione, R.A. (1998). Characterization of the association of the actin-binding protein, IQGAP, and activated Cdc42 with Golgi membranes. J. Biol. Chem. *273*, 22537–22544.

Min, J., Okada, S., Kanzaki M., Elmendorf, J.S., Coker, K.J., Ceresa, B.P., Syu, L.J., Noda., Y., Saltiel, A.R. and Pressin, J.E. (1999). Synip: a novel insulin-regulated syntaxin 4-binding protein mediating GLUT4 translocation in adipocytes. Mol. Cell. *3*, 751–760.

Moreau, V., Frischknecht, F., Reckmann, I., Vincentelli, R., Rabut, G., Stewart, D., and Way, M. (2000). A complex of N-WASP and WIP integrates signaling cascades that lead to actin polymerization. Nat. Cell Biol. *2*, 441–448.

Moreau, V., and Way, M. (1998). Cdc42 is required for membrane dependent actin polymerization in vitro. FEBS Lett. *427*, 353–356.

Morita, K., Oka, M., and Hamano, S. (1988). Effects of cytoskeleton-disrupting drugs on ouabain-stimulated catecholamine secretion from cultured adrenal chromaffin cells. Biochem. Pharmacol. *37*, 3357–3359.

Morton, W.M., Ayscough, K.R., and McLaughlin, P.J. (2000). Latrunculin alters the actin-monomer subunit interface to prevent polymerization. Nat. Cell Biol. *2*, 376–378.

Muallem, S., Kwiatkowska, K., Xu, X., and Yin, H.L. (1995). Actin filament disassembly is a sufficient final trigger for exocytosis in nonexcitable cells. J. Cell Biol. *128*, 589–598.

Murphy, G.A., Solski, P.A., Jillian, S.A., Perez de la Ossa, P., D'Eustachio, P., Der, C.J., and Rush, M.G. (1999). Cellular functions of TC10, a Rho family GTPase: regulation of morphology, signal transduction and cell growth. Oncogene *18*, 3831–3845.

Murray, A.W., and Kirschner, M.W. (1989). Cyclin synthesis drives the early embryonic cell cycle. Nature *339*, 275–280.

Musch, A., Cohen, D., Kreitzer, G., and Rodriguez-Boulan, E. (2001). Cdc42 regulates the exit of apical and basolateral proteins from the trans-Golgi network. EMBO J. *20*, 2171–2179.

Musch, A., Cohen, D., and Rodriguez-Boulan, E. (1997). Myosin II is involved in the production of constitutive transport vesicles from the TGN. J. Cell Biol. *138*, 291–306.

Nehls, S., Snapp, E.L., Cole, N.B., Zaal, K.J., Kenworthy, A.K., Roberts, T.H., Ellenberg, J., Presley, J.F., Siggia, E., and Lippincott-Schwartz, J. (2000). Dynamics and retention of misfolded proteins in native ER membranes. Nat. Cell Biol. *2*, 288–295.

Neudauer, C.L., Joberty, G., Tatsis, N., and Macara, I.G. (1998). Distinct cellular effects and interactions of the Rho-family GTPase TC10. Curr. Biol. *8*, 1151–1160.

Nobes, C.D., and Hall, A. (1995). Rho, rac, and cdc42 GTPases regulate the assembly of multimolecular focal complexes associated with actin stress fibers, lamellipodia, and filopodia. Cell *81*, 53–62.

Norman, J.C., Price, L.S., Ridley, A.J., and Koffer, A. (1996). The small GTP-binding proteins, Rac and Rho, regulate cytoskeletal organization and exocytosis in mast cells by parallel pathways. Mol. Biol. Cell *7*, 1429–1442.

O'Konski, M.S., and Pandol, S.J. (1990). Effects of caerulein on the apical cytoskeleton of the pancreatic acinar cell. J. Clin. Invest. *86*, 1649–1657.

O'Konski, M.S., and Pandol, S.J. (1993). Cholecystokinin JMV-180 and caerulein effects on the pancreatic acinar cell cytoskeleton. Pancreas *8*, 638–646.

Omata, W., Shibata, H., Li, L., Takata, K., and Kojima, I. (2000). Actin filaments play a critical role in insulin-induced exocytotic recruitment but not in endocytosis of GLUT4 in isolated rat adipocytes. Biochem. J. *346*, 321–328.

Presley, J.F., Cole, N.B., Schroer, T.A., Hirschberg, K., Zaal, K.J., and Lippincott-Schwartz, J. (1997). ER-to-Golgi transport visualized in living cells. Nature *389*, 81–85.

Ridley, A.J., and Hall, A. (1992). The small GTP-binding protein rho regulates the assembly of focal adhesions and actin stress fibers in response to growth factors. Cell *70*, 389–399.

Ridley, A.J., Paterson, H.F., Johnston, C.L., Diekmann, D., and Hall, A. (1992). The small GTP-binding protein rac regulates growth factor-induced membrane ruffling. Cell *70*, 401–410.

Sontag, J.M., Aunis, D., and Bader, M.F. (1988). Peripheral actin filaments control calcium-mediated catecholamine release from streptolysin-O-permeabilized chromaffin cells. Eur J. Cell Biol. *46*, 316–326.

Suzuki, T., Miki, H., Takenawa, T., and Sasakawa, C. (1998). Neural Wiskott-Aldrich syndrome protein is implicated in the actin-based motility of *Shigella flexneri*. EMBO J. *17*, 2767–2776.

Suzuki, T., Mimuro, H., Miki, H., Takenawa, T., Sasaki, T., Nakanishi, H., Takai, Y., and Sasakawa, C. (2000). Rho family GTPase Cdc42 is essential for the actin-based motility of *Shigella* in mammalian cells. J. Exp. Med. *191*, 1905–1920.

Taunton, J., Rowning, B.A., Coughlin, M.L., Wu, M., Moon, R.T., Mitchison, T.J., and Larabell, C.A. (2000). Actin-dependent propulsion of endosomes and lysosomes by recruitment of N-WASP. J. Cell Biol. *148*, 519–530.

Tong, P., Khayat, Z.A., Huang, C., Patel, N., Ueyama, A., and Klip, A. (2001). Insulin-induced cortical actin remodeling promotes GLUT4 insertion at muscle cell membrane ruffles. J. Clin. Invest. *108*, 371–381.

Tsakiridis, T., Bergman, A., Somwar, R., Taha, C., Aktories, K., Cruz, T.F., Klip, A., and Downey, G.P. (1998). Actin filaments facilitate insulin activation of the src and collagen homologous/mitogen-activated protein kinase pathway leading to DNA synthesis and c-fos expression. J. Biol. Chem. *273*, 28322–28331.

Tsakiridis, T., Vranic, M., and Klip, A. (1994). Disassembly of the actin network inhibits insulin-dependent stimulation of glucose transport and prevents recruitment of glucose transporters to the plasma membrane. J. Biol. Chem. *269*, 29934–29942.

Valderrama, F., Duran, J.M., Babia, T., Barth, H., Renau-Piqueras, J., and Egea, G. (2001). Actin microfilaments facilitate the retrograde

transport from the Golgi complex to the endoplasmic reticulum in mammalian cells. Traffic *2*, 717–726.

Valderrama, F., Luna, A., Babia, T., Martinez-Menarguez, J.A., Ballesta, J., Barth, H., Chaponnier, C., Renau-Piqueras, J., and Egea, G. (2000). The Golgi-associated COPI-coated buds and vesicles contain beta/gamma-actin. Proc. Natl. Acad. Sci. USA *97*, 1560–1565.

Vitale, M.L., Rodriguez Del Castillo, A., Tchakarov, L., and Trifaro, J.M. (1991). Cortical filamentous actin disassembly and scinderin redistribution during chromaffin cell stimulation precede exocytosis, a phenomenon not exhibited by gelsolin. J. Cell Biol. *113*, 1057–1067.

Vitale, M.L., Seward, E.P., and Trifaro, J.M. (1995). Chromaffin cell cortical actin network dynamics control the size of the release-ready vesicle pool and the initial rate of exocytosis. Neuron *14*, 353–363.

Wang, Q., Bilan, P.J., Tsakiridis, T., Hinek, A., and Klip, A. (1998). Actin filaments participate in the relocalization of phosphatidylinositol3-kinase to glucose transporter-containing compartments and in the stimulation of glucose uptake in 3T3–L1 adipocytes. Biochem. J. *331*, 917–928.

Watson, R.T., Shigematsu, S., Chiang, S.H., Mora, S., Kanzaki, M., Macara, I.G., Saltiel, A.R., and Pessin, J.E. (2001). Lipid raft microdomain compartmentalization of TC10 is required for insulin signaling and GLUT4 translocation. J. Cell Biol. *154*, 829–840.

Westphal, M., Jungbluth, A., Heidecker, M., Muhlbauer, B., Heizer, C., Schwartz, J.M., Marriott, G., and Gerisch, G. (1997). Microfilament dynamics during cell movement and chemotaxis monitored using a GFP-actin fusion protein. Curr. Biol. *7*, 176–183.

Wu, W.J., Erickson, J.W., Lin, R., and Cerione, R.A. (2000). The gamma-subunit of the coatomer complex binds Cdc42 to mediate transformation. Nature *405*, 800–804.

Yamauchi, K., and Pessin, J.E. (1994). Insulin receptor substrate-1 (IRS1) and Shc compete for a limited pool of Grb2 in mediating insulin downstream signaling. J. Biol. Chem. *269*, 31107–31114.